11. T. Abe, K. Koyano, H. Saisu, Y. Nishiuchi, S. Sakakibara, *Neurosci. Lett.* **71**, 203 (1991); L. J. Cruz and B. M. Oliveria, *J. Biol. Chem.* **261**, 6230 (1986).
12. Scatchard binding analysis was performed on the purified receptor as described (*23*) with use of polyethylenimine-presoaked Whatman GFB filters. Nonspecific binding (less than 10%) was determined in the presence of 5 μM unlabeled ω-conotoxin.
13. Sucrose gradient fractions were separated by SDS-PAGE on 3 to 12% linear gradient gels and transferred to nitrocellulose (150 μl per lane) [K. P. Campbell and S. D. Kahl, *Nature* **338**, 259 (1989)]. Specific polyclonal antibodies against the α_1, α_2, 95K, and β subunits were affinity-purified as described by J. M. Ervasti and K. P. Campbell [*Cell* **66**, 1121 (1991)].
14. Monoclonal and affinity-purified sheep polyclonal antibodies were coupled to protein G–agarose. Rabbit brain membranes (2 mg per milliliter of solution) labeled with 0.5 nM ^{125}I-labeled ω-conotoxin or 10 nM [^{3}H]PN200-110 were solubilized as previously described (*23*). The percent of ^{125}I-labeled ω-conotoxin or [^{3}H]PN200-110 binding sites immunoprecipitated was determined by either gamma or scintillation counting. Nonspecific binding of [^{3}H]PN200-110 was measured in the presence of 10 μM nitrendipine.
15. The SDS-PAGE was carried out on 3 to 12% gradient gels in the presence of 1% 2-mercaptoethanol. Skeletal muscle DHP receptor was purified as described by S. D. Jay *et al.* [*J. Biol. Chem.* **266**, 3287 (1991)].
16. Four peptide sequences from the 140-kD subunit (reduced form of the 160-kD subunit) of the ω-conotoxin receptor clearly identified it as a neuronal α_2 subunit. Deglycosylation of the ω-conotoxin receptor complex was performed as previously described [J. B. Parys *et al.*, *J. Biol. Chem.* **267**, 18776 (1992)]. The α_{1B} glutathione-S-transferase (GST) fusion protein consisted of amino acid residues 720 to 1139 [S. J. Dubel *et al.*, *Proc. Natl. Acad. Sci. U.S.A.* **89**, 5058 (1992)] and was produced as described in (*24*). Affinity-purified antibodies against the ω-conotoxin receptor β subunit were used to screen a lambda gt11 rat brain cDNA expression library. A full-length β_3 clone, highly homologous to the β_3 clone sequenced by Hullin *et al.*, (*22*), was obtained. A COOH-terminal (residues 369 to 484) GST fusion protein unique to the β_3 and an NH_2-terminal (residues 9 to 296) GST fusion protein, which contains regions highly homologous to all of the β subunits, were produced as described in (*24*). Polyclonal antibodies to a peptide specific to the β_1 subunit did not recognize the ω-conotoxin receptor.
17. The tip-dip technique was preferred over the standard technique of painted lipid bilayers because it has a smaller membrane capacitance and an improved signal-to-noise ratio, which makes the tip-dip method better suited for resolving fast gating and low-amplitude channels. A bovine brain phospholipid mixture (10 μl) (phosphatidylethanolamine:phosphatidylserine with a weight ratio of 1:1; Avanti Polar Lipids) at 30 mg per milliliter of decane was spread on the surface of a 2-ml bath. Bilayer membranes were formed by the apposition of two monolayers at the tip of fire-polished and Sylgard-coated patch electrodes of mean resistance 7 megohms (n = 27). Bilayers with seal resistances below 10 gigohms were discarded to avoid possible artifacts. The solution on both sides of the bilayer (symmetrical ionic conditions) contained (Fig. 3, A and C) 100 mM $BaCl_2$ and 10 mM Hepes-tris (pH 7.4) or (Fig. 3B) 10 mM $BaCl_2$ and 1 mM Hepes-tris (pH 7.4). Before reconstitution, the purified receptor was phosphorylated by calcium-calmodulin dependent protein kinase II (CaM kinase II) to increase channel activity. The reaction medium contained 10 mM Hepes (pH 7.4), 0.3 M NaCl, 5 mM $MgCl_2$, 1 mM $CaCl_2$, 1 mM EGTA, 1 mM adenosine triphosphate, 7% sucrose, 0.05% digitonin, and 10 μg of calmodulin, 0.5 μg of CaM kinase II, and 12.5 nmol of receptor per milliliter of solution. The potential across the bilayer was controlled by clamping the electrode potential with respect to the bath. By convention, as provided by the Axopatch 200A (Axon Instruments), a negative current is defined by the net cation flow from the bath to the pipette. Chloride current flow in the opposite direction was excluded by current-reversal potential measurements after a decrease in $BaCl_2$ concentration in the bath. Average unitary currents were constructed before and after drug application with the following protocol applied every three seconds: the steady-state voltage [(B) −100 mV, (C) +100 mV] was transiently stepped to 0 mV (reversal potential) for 50 ms and stepped back to the same potential for 300 ms [between arrows, last traces of (B) and (C)]. Recordings were low-pass–filtered at a corner frequency of 1 kHz with an 8-pole Bessel filter and were computer-digitized at 5 kHz. Traces were leak subtracted, and electrode capacitance was compensated.
18. R. Coronado and R. Latorre, *Biophys. J.* **43**, 231 (1983).
19. V. Flockerzi *et al.*, *Nature* **323**, 66 (1986).
20. A. P. Fox, M. C. Nowycky, R. W. Tsien, *J. Physiol. (London)* **394**, 173 (1987); M. R. Plummer, D. E. Logothetis, P. Hess, *Neuron* **2**, 453 (1989).
21. A. J. Wagner, A. M. Snowman, A. Biswas, B. M. Olivera, S. H. Snyder, *J. Neurosci.* **8**, 3354 (1988); M. K. Ahlijanian, J. Striessnig, W. A. Catterall, *J. Biol. Chem.* **266**, 20192 (1991); M. W. McEnery, A. M. Snowman, A. H. Sharp, M. E. Adams, S. H. Snyder, *Proc. Natl. Acad. Sci. U.S.A.* **88**, 11095 (1991).
22. R. Hullin *et al.*, *EMBO J.* **11**, 885 (1992).
23. J. Sakamoto and K. P. Campbell, *J. Biol. Chem.* **266**, 18914 (1991).
24. O. Ibraghimov-Beskrovnaya *et al.*, *Nature* **355**, 696 (1992).
25. P. S. McPherson *et al.*, *Neuron* **7**, 17 (1991).
26. We would like to thank T. Snutch for the brain α_{1B} cDNA clone and H. Schulman for the CaM kinase II. K.P.C. is an investigator of the Howard Hughes Medical Institute.

25 March 1993; accepted 27 May 1993

How Somatotopic Is the Motor Cortex Hand Area?

Marc H. Schieber* and Lyndon S. Hibbard

The primary motor cortex (M1) is thought to control movements of different body parts from somatotopically organized cortical territories. Electrical stimulation suggests, however, that territories controlling different fingers overlap. Such overlap might be artifactual or else might indicate that activation of M1 to produce a finger movement occurs over a more widespread cortical area than usually assumed. These possibilities were distinguished in monkeys moving different fingers. Recordings showed that single M1 neurons were active with movements of different fingers. Neuronal populations active with movements of different fingers overlapped extensively. Control of any finger movement thus appears to utilize a population of neurons distributed throughout the M1 hand area rather than a somatotopically segregated population.

Icons summarizing the somatotopy of M1, such as Penfield's homunculus or Woolsey's simiusculus, imply that spatially separate cortical territories control the movements of different body parts, with separate territories for each digit of the primate hand (*1*). Yet these and other early investigations demonstrated that in the hand area, where a relatively large expanse of cortex is devoted to a relatively small portion of the body, the cortical territories where surface stimulation evoked movements of different digits overlapped considerably (*1*, *2*). Recent studies with intracortical microstimulation, which provides cortical excitation more focal than previously available, have continued to show overlap of the cortical territories where stimulation elicits contractions of different muscles (*3*) or movements of different fingers (*4*). Mapping M1 with electrical stimulation, however, may not accurately mimic the natural neuronal activity underlying finger movements. To distinguish whether separate or overlapping territories are activated during movements of different fingers (*5*), we studied the spatial distribution of single-neuron activity in M1 during finger movements performed by awake monkeys.

Two rhesus monkeys were trained to perform visually cued individuated flexion and extension movements of each digit of the right hand and of the right wrist (*6*). In each correctly performed trial, the digit the monkey had been instructed to move (the instructed digit) underwent more movement than any other (noninstructed) digit. In some movements, particularly when the monkey was instructed to flex the thumb, noninstructed digits remained stationary; in other movements, noninstructed digits moved to varying degrees. Therefore, each movement is referred to as an instructed movement of a given digit because lesser movement of noninstructed digits often occurred (*7*–*9*). Nevertheless, as the instructed digit was varied in different trials from the thumb to the little finger, the

M. H. Schieber, Departments of Neurology and Neurosurgery (Neurology) and of Anatomy and Neurobiology, Washington University School of Medicine, St. Louis, MO 63110.
L. S. Hibbard, Department of Neurology and Neurosurgery (Neurology), Washington University School of Medicine, St. Louis, MO 63110.
*To whom correspondence should be addressed.

subset of digits that moved progressed systematically from the radial to the ulnar digits.

For 136 M1 neurons in monkey K and 84 neurons in monkey S, spike discharge data were collected during four or more correctly performed trials of each of the 12 instructed movements (*10*). Of these, 115 neurons in monkey K and 61 in monkey S were significantly and consistently related to at least 1 of the 12 instructed movements (*11, 12*). Although some neurons were related to just one instructed movement, many neurons were related to more than one. The neuron shown, for example, changed its firing frequency most with instructed movement 3e, but was also related to 3f, 4f, Wf, 1e, 2e, 4e, 5e, and We (Fig. 1). Indeed, the majority of neurons were related to two or more instructed movements (Fig. 2). The relation of single M1 neurons to multiple instructed movements suggested that during any given instructed movement, active neurons would be found over a considerable portion of the M1 hand area.

We therefore reconstructed the M1 hand area of each monkey to study the spatial distribution of activity in all recorded neurons during each instructed movement (Fig. 3) (*13*). M1 neurons related to finger movements were found in the anterior bank and lip of the central sulcus. Here, according to the classic M1 simiusculus (or homunculus), the digits should be represented in a lateromedial sequence, with the thumb lateral and the little finger medial (*1*). This implies that neurons active during thumb movements should be found most lateral, neurons active during little finger movements most medial, and neurons active during movements of other fingers should be arrayed sequentially in between. But displaying the spatial distribution of changes in neuronal activity during different instructed movements demonstrated that active neurons were distributed throughout the hand area during each instructed movement (Fig. 3B). Though activity during instructed thumb flexion (1f) appeared more intense laterally, separate territories of active neurons progressing from lateral to medial as the instructed digit was varied from thumb through little finger were not evident for either flexion or extension movements. Moreover, though the simiusculus suggests that wrist and digit movements are represented separately, the territory of neurons related to wrist movements (Wf and We) appeared coextensive with the territories for finger movements. Similar observations were made in monkey S (not shown). The spatial distribution of M1 single-neuron activity during different instructed movements was examined further in three ways.

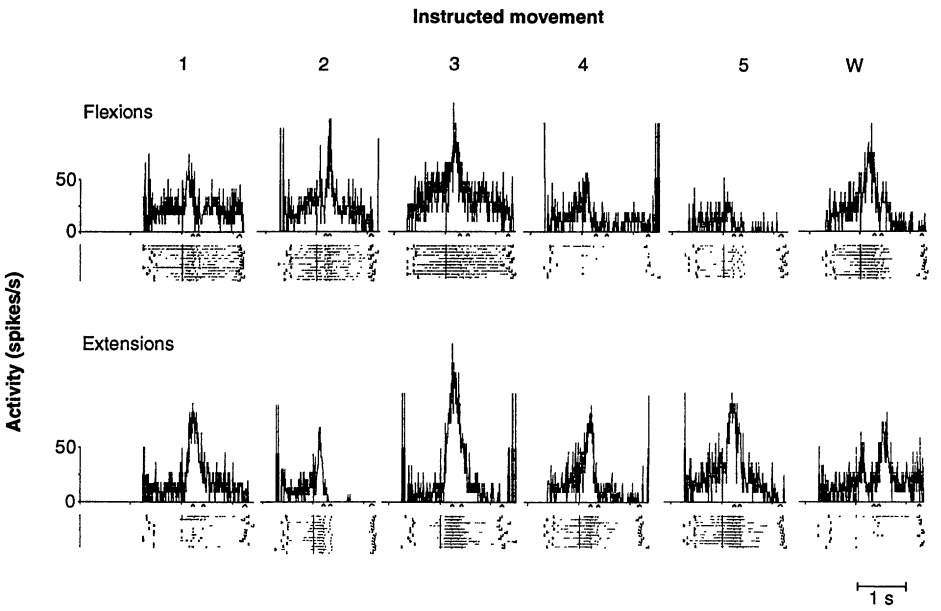

Fig. 1. Activity of an M1 neuron during finger movements. The traces show activity during instructed flexion (upper row) and during instructed extension (lower row) of each digit. In each frame, the dot raster below shows the neuron's discharge during 10 to 13 successful trials of the indicated instructed movement, aligned at the onset of the instruction signal (vertical line); the peri-event histogram above is formed from this rastered data (bin width, 10 ms). Tick marks in each raster line indicate (i) movement onset in the instructed digit, (ii) end of movement, and (iii) reward delivery; carat marks beneath each histogram indicate the average time of these events.

First, we displayed each neuron's "best" instructed digit as a sphere of radius proportional to the neuron's greatest discharge frequency change for any of the 12 instructed movements, and of color representing the instructed digit associated with that change (Fig. 3C, Max). Though neurons best related to thumb movements (red spheres) were slightly concentrated laterally, and neurons best related to little finger movements (blue spheres) were slightly concentrated medially, neurons best related to instructed movements of different digits were intermingled throughout the hand area.

Second, using the data displayed in each panel in Fig. 3B, we calculated the centroid of activity for each instructed movement (Fig. 3C, Cent). Though the population of neurons in monkey K extended more than 8 mm along the central sulcus, the centroids for the 12 instructed movements were all clustered within 2 mm. Similarly in monkey S, the population extended 9 mm along the central sulcus, yet the 12 centroids were clustered in the central 2 mm. This clustering further indicates the spatial overlap of neurons active during instructed movements of different fingers.

Third, to evaluate systematic progression of activity lateromedially along the central sulcus during movements of different fingers, we correlated instructed digit number (1 to 5) with the projected location of the centroids along a line tangential to the central sulcus (*14*). Spearman's rank correlation coefficient (r_s) was insignificant

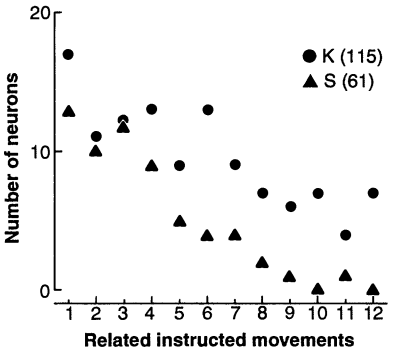

Fig. 2. Plots of the number of M1 neurons (totals in parentheses) related to different numbers of instructed movements in monkeys K and S.

in monkey S ($r_s = 0.00$, $n = 10$, $P > 0.05$) but attained significance in monkey K ($r_s = 0.69$, $n = 10$, $P < 0.05$). For monkey K we therefore linearly regressed the centroids' projected locations against instructed digit number, obtaining a slope estimate of 0.16 mm average progression along the central sulcus per digit, an order of magnitude less than would be predicted if each digit had a separate representation along the 8 mm of M1 hand region (8 mm per five digits = 1.6 mm per digit).

The present findings emphasize the spatial overlap of cortical territories for movements of different fingers. In part, this overlap could reflect cortical activation either to move or to stabilize noninstructed digits. But the conceptually distinct, though not necessarily operationally sepa-

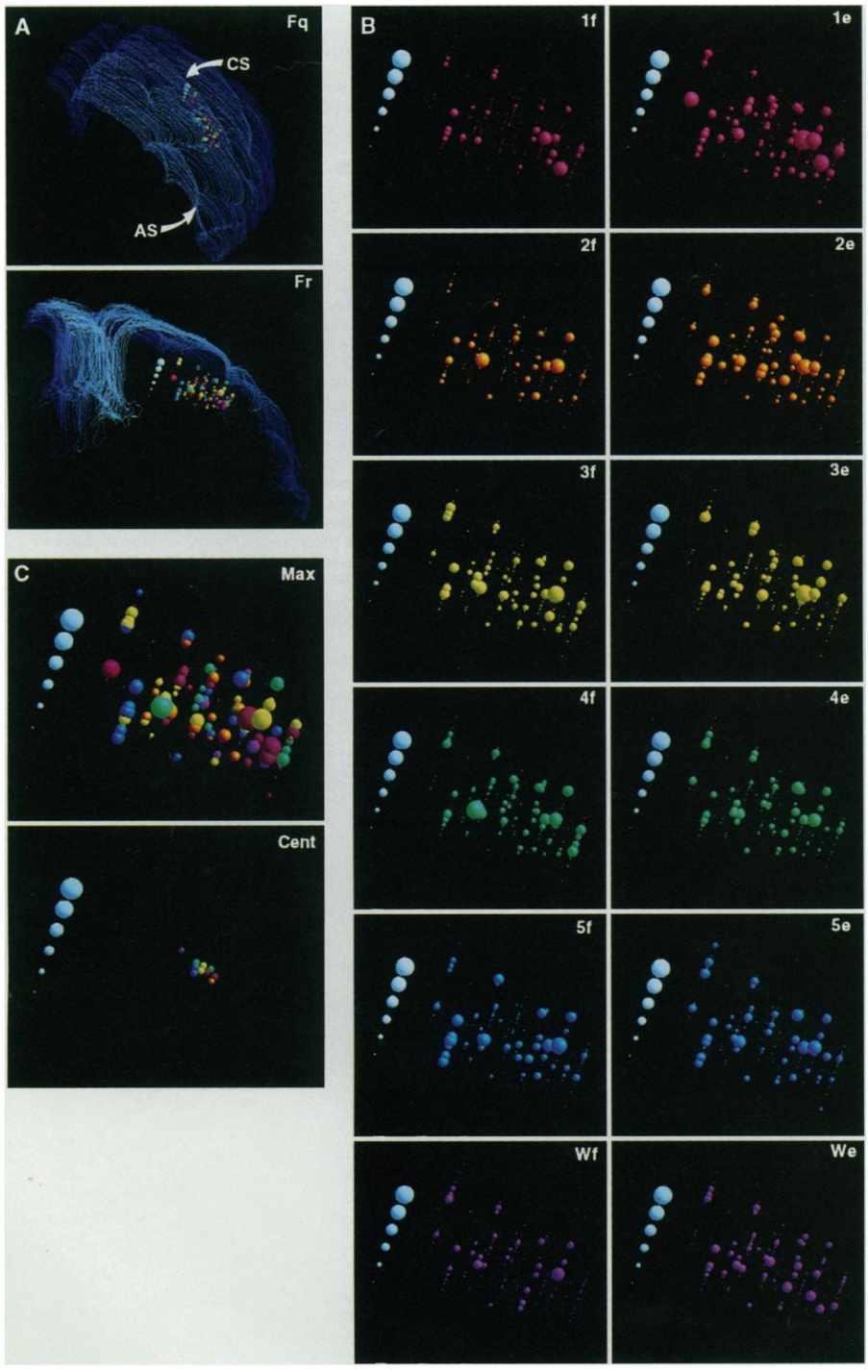

Fig. 3. Distribution of neuronal activity in M1 of monkey K during individuated finger movements. (**A**) Orienting views of the reconstructed left hemisphere block. The forequarter view (Fq) shows surface features, including the central sulcus (CS) and arcuate sulcus (AS, arrow points at lower limb). The view from the frontal pole (Fr) shows the population of M1 neurons as spheres beneath the surface convexity, with the midline interhemispheric fissure seen to the left. (**B**) Distribution of single-neuron activity during the 12 instructed movements. Frames of (B) and (C) all show the population in the frontal pole orientation: surface convexity above, medial left, lateral right. In each frame of (B), each recorded M1 neuron is represented by a sphere centered at the reconstructed coordinates of that neuron, colored according to the instructed digit (red, orange, yellow, green, blue, and violet for digits 1, 2, 3, 4, and 5 and Wrist, respectively). The radius of each sphere is proportional to that neuron's change in discharge frequency during that instructed movement. Neurons not related to a given instructed movement are shown as points. (**C**) Each sphere is sized to represent the maximal change in discharge frequency (Max) for that neuron during any of the 12 instructed movements and colored to represent the instructed digit for that particular movement. The centroids (Cent) for each instructed movement are calculated from the data shown in the 12 frames of (B). White spheres in each frame constitute a scale: Centers are 1 mm apart (in the direction of electrode travel), and radii represent changes in firing frequency of 0, 40, 80, 120, 160, and 200 spikes per s.

rate, processes of moving the instructed digit and of stabilizing noninstructed digits may involve M1 simultaneously (*5*, *15*). Moreover, given (i) that territories where cortical stimulation evokes movements of different digits (*1*, *2*, *4*) or contractions of different finger muscles (*3*), or where cortical neurons receive afferent input from different fingers (*16*), all overlap; (ii) that many cortical neurons influence more than one finger muscle (*17*); and (iii) that widespread horizontal connections exist throughout the M1 hand area (*18*), the overlapping cortical territories active during different finger movements cannot simply be attributed to control of noninstructed digits. Rather than being specified by a somatotopic map, each finger movement, like each movement direction (*19*), appears to be specified by a neuronal population distributed throughout the M1 hand area.

REFERENCES AND NOTES

1. W. Penfield and T. Rasmussen, *The Cerebral Cortex of Man* (Macmillan, New York, 1950); C. N. Woolsey *et al.*, *Res. Publ. Assoc. Res. Nerv. Ment. Dis.* **30**, 238 (1951).
2. A. S. F. Leyton and C. S. Sherrington, *Q. J. Exp. Physiol.* **11**, 137 (1917); W. Penfield and E. Boldrey, *Brain* **37**, 389 (1937); C. N. Woolsey, T. C. Erickson, W. E. Gilson, *J. Neurosurg.* **51**, 476 (1979).
3. P. Andersen, P. J. Hagan, C. G. Phillips, T. P. S. Powell, *Proc. R. Soc. London Ser. B* **188**, 31 (1975); H. Asanuma and I. Rosen, *Exp. Brain Res.* **14**, 243 (1972); J. P. Donoghue, S. Leibovic, J. N. Sanes, *ibid.* **89**, 1 (1992); D. R. Humphrey, *Fed. Proc.* **45**, 2687 (1986); K. C. Sato and J. Tanji, *J. Neurophysiol.* **62**, 959 (1989); R. S. Waters, D. D. Samulack, R. W. Dykes, P. A. McKinley, *Somatosens. Mot. Res.* **7**, 485 (1990).
4. H. J. Gould, C. G. Cusick, T. P. Pons, J. H. Kaas, *J. Comp. Neurol.* **247**, 297 (1986); H. C. Kwan, W. A. MacKay, J. T. Murphy, Y. C. Wong, *J. Neurophysiol.* **41**, 1120 (1978); P. L. Strick and J. B. Preston, *Brain Res.* **154**, 366 (1978).
5. M. H. Schieber, *Trends Neurosci.* **13**, 440 (1990).
6. ———, *J. Neurophysiol.* **65**, 1381 (1991).
7. For brevity, each instructed movement is denoted by the number of the instructed digit (1 for thumb through 5 for little finger, and W for wrist) and the instructed direction (f, flexion; e, extension); 2e thus denotes instructed extension of the index finger.
8. The structure of macaque finger muscles [D. M. Serlin and M. H. Schieber, *Acta Anat.* **146**, 225 (1993)] and the fact that training each monkey required more than 1 year suggest that the degree of independence of the present finger movements, described quantitatively in (*6*), approaches the limits of independence for macaques.

9. Similar movements of noninstructed digits are typical of skilled human typists [J. Fish and J. F. Soechting, *Exp. Brain Res.* **91**, 327 (1992); M. Flanders and J. F. Soechting, *J. Neurophysiol.* **67**, 1264 (1992)].
10. All procedures for the care and use of monkeys conformed to the guidelines of the Animal Studies Committee of Washington University. Under intravenous thiopental anesthesia (20 to 30 mg/kg) and with aseptic surgical technique, each monkey was prepared for recording by implantation of a rectangular lucite chamber over a craniotomy that exposed the M1 hand area. Extracellular action potentials were recorded with transdural, glass-coated Pt-Ir microelectrodes advanced with a Trent-Wells hydraulic microdrive mounted on a custom XYZ micropositioner, which was attached to the lucite chamber. Trials of different instructed movements were presented in a pseudorandom rotation.
11. For each correctly performed trial, the spike count in 10-ms bins was smoothed with a 50-ms window, and a Kolmogorov-Smirnov test was used to evaluate differences between the distributions of counts per bin during a control period (500 ms preceding the instruction) and each of three periods (the premovement period, the movement period, and the total reaction time period) at the $P < 0.05$ level. (The 50-ms period after the onset of the instruction light-emitting diode, during which time no activity changes were observed in any M1 neurons, was excluded from these tests to maximize sensitivity.) A neuron was considered to have discharged consistently in relation to an instructed movement if its discharge during any one of the three test periods was significantly different from its discharge during the control period in 90% or more of the correctly performed trials. If so related, the change in that neuron's firing frequency for that instructed movement was calculated as the difference between the peak (or trough) during the total reaction time and the average discharge during the control period. If not related, the neuron's change for that movement was assigned a value of 0.
12. Some M1 neurons respond to visual stimuli [T. M. J. Wannier, M. A. Maier, M.-C. Hepp-Reymond, *Neurosci. Lett.* **98**, 63 (1989)]. Because responses to the visual cues were rare in the present data and did not occur with similar visual stimuli that did not elicit trained finger movements, visual responses were unlikely to affect the present analysis.
13. Digitized images of Nissl-stained tissue sections were computationally aligned [L. S. Hibbard and R. A. Hawkins, *J. Neurosci. Methods* **26**, 55 (1988)], and selected surface and sulcal contours were displayed. Selected electrode penetration tracks were traced through sequential histologic-digitized tissue sections and were displayed. The microdrive-micropositioner *XYZ* coordinates along all electrode penetrations were then displayed as a separate graphical object of which the positioning was adjusted visually to fit the reconstructed penetration tracks and contours. This coordinate system was used to locate each recorded neuron within the reconstructed tissue block. Computer graphics were developed with GRAMPS software [T. J. O'Donnell and A. J. Olsen, *Comput. Graphics* **15**, 133 (1981)].
14. Because the wrist is not typically assumed to be represented in line with digits 1 to 5, the centroids for wrist movements (Wf and We) were excluded from this calculation (*1–4*).
15. D. R. Humphrey, *Electroencephalogr. Clin. Neurophysiol. Suppl.* **36**, 393 (1982); _____ and D. J. Reed, in *Motor Control Mechanisms in Health and Disease*, J. E. Desmedt, Ed. (Raven, New York, 1983), p. 347.
16. Y. C. Wong, H. C. Kwan, W. A. MacKay, J. T. Murphy, *J. Neurophysiol.* **41**, 1107 (1978); R. N. Lemon, *J. Physiol.* **311**, 521 (1981).
17. E. J. Buys, R. N. Lemon, G. W. H. Mantel, R. B. Muir, *J. Physiol.* **381**, 529 (1986); E. E. Fetz and P. D. Cheney, *J. Neurophysiol.* **44**, 751 (1980); Y. Shinoda, J. Yokota, T. Futami, *Neurosci. Lett.* **23**, 7 (1981).
18. J. DeFelipe, M. Conley, E. G. Jones, *J. Neurosci.* **6**, 3749 (1986); G. W. Huntley and E. G. Jones, *J. Neurophysiol.* **66**, 390 (1991).
19. A. P. Georgopoulos, A. B. Schwartz, R. E. Kettner, *Science* **223**, 1416 (1986).
20. We thank W. T. Thach for helpful discussions, J. McCausland for use of his digitizing camera, T. Anderson and B. McClure for histology, M. Hayles for editorial assistance, and B. Forgash for manuscript preparation. Preliminary results have been presented [M. H. Schieber, *Soc. Neurosci. Abstr.* **18**, 504 (1992)]. Supported by National Institute of Neurological Diseases and Stroke grant RO1-NS27686.

13 January 1993; accepted 19 May 1993